PAN
POLSKA AKADEMIA NAUK

M&MS

ELECTROCHEMICAL SENSORS BASED ON TiO$_2$–Fe$_2$O$_3$ COUPLED SYSTEM

Anna Kusior[1], Iwona Karoń[2], Marta Radecka[1]

1) *AGH University of Science and Technology, Faculty of Materials Science and Ceramics, al. Mickiewicza 30, 30-059 Kraków, Poland* (✉ *akusior@agh.edu.pl,* +48 22 617 2468)

2) *University of Applied Sciences in Tarnow, Faculty of Mathematical and Natural Sciences, ul. Mickiewicza 8, 33-100 Tarnów, Poland*

Abstract

Recently, transition metal oxides, which exhibit favorable catalytic abilities, have also been investigated as a material for the detection of hydrazine (N$_2$H$_4$). It has been reported that mixed metal oxides usually offer a higher electrochemical activity than binary oxides. In this work, a TiO$_2$–Fe$_2$O$_3$ coupled system is presented as an enhanced material with major applications in electrochemical detectors. The electrochemical behavior of glassy carbon electrodes modified with TiO$_2$–Fe$_2$O$_3$ in the absence and presence of hydrazine was evaluated via cyclic voltammetry (CV). Experimental results also suggest that the formation of the TiO$_2$–Fe$_2$O$_3$ coupled system enhances electrochemical catalytic performance in N$_2$H$_4$ detection. The modification TiO$_2$ + 2 mol% Fe$_2$O$_3$ provides good analytical performance of detection (0.13 mM) and quantification limits (0.39 mM). The presented coupled system provides the premise for a suitable material for a stable and sensitive N$_2$H$_4$ sensor.

Keywords: electrochemical sensor, cyclic voltammetry, hydrazine, TiO$_2$, Fe$_2$O$_3$.

1. Introduction

Hydrazine (N$_2$H$_4$) and its derivative compounds are widely used in agriculture as well as the chemical and pharmaceutical industries, with application as antioxidants, emulsifiers, insecticides, plant-growth regulators, corrosion inhibitors, and catalysts in fuel for aircraft and satellites [1–3]. In spite of its importance, hydrazine has been reported to act as a carcinogen, hepatotoxin and neurotoxin which damages the lungs, liver, kidneys, brain, DNA and also causes an irreversible deterioration of the nervous system [4]. In addition, hydrazine and its derivatives contribute to environmental pollution.

The maximum recommended level of hydrazine in trade effluents is 1 ppm [5, 6]. Accurate and sensitive hydrazine detection procedures are, therefore, absolutely, indispensable. Numerous instrumental methods have been applied to determine N$_2$H$_4$, including potentiometry, spectrophotometry, fluorescence, and chromatography [7–12]. Of such methods, the electrochemical technique has been considered particularly attractive owing to its high sensitivity, good selectivity,

fast response, simple instrumentation and low cost [13, 14]. The electroanalysis of hydrazine is based on its direct oxidation on the electrode surface. However, the determination of N_2H_4 on an unmodified electrode is restricted by a very low reaction rate, large overpotentials and small oxidation currents [15, 16]. In order to improve its analytical properties, chemical modifications of inert electrodes have been extensively explored. Many sensing materials, such as metallic nanoparticles, conducting polymers, or nano-carbon based materials, have been developed to allow the fabrication of non-enzymatic hydrazine sensors [17–20]. Recently, transition metal oxides, which exhibit favourable catalytic abilities, have also been investigated as a material for the detection of N_2H_4. It has been reported that mixed metal oxides usually offer higher electrochemical activity than binary oxides [21–24]. It appears that such systems benefit from the combination of the best properties of their pure components and that the electronic structure of the system can be expected to change as a result. Titanium dioxide (TiO_2), which exhibits good chemical and thermal stability, ion-changeable ability, and biocompatibility, is one of the most promising semiconductors in this respect. The prerequisite for the optimal performance of titania is the selection of an appropriate supporting material [25–27] which yields a possible synergetic effect and thus contributes to the enhancement of electrocatalytic activity.

In this work, a TiO_2–Fe_2O_3 coupled system is presented as an enhanced material with major applications in electrochemical sensors of hydrazine [28–30].

2. Experimental

2.1. Synthesis procedure

The sol-gel technique was applied to obtain a series of TiO_2–Fe_2O_3 mixed oxide powders with different Ti:Fe molar ratios. The TiO_2–Fe_2O_3 coupled system was prepared by means of a modified synthetic procedure proposed by Kundu *et al*. [31]. Powders based on titanium dioxide were prepared from tertaisopropyl orthotitanate ($C_{12}H_{28}O_4Ti$, Fluka) and iron (III) nitrate nonahydrate ($Fe(NO_3)_3 \times H_2O$, Fluka) as precursors. The sol of titania was obtained via the hydrolysis of $C_{12}H_{28}O_4Ti$ in a mixture of acetic acid and ethyl alcohol (in a volume ratio of $1:3$). After mixing at room temperature for 1 h, an aqueous solution of $Fe(NO_3)_3$ was added and stirring continued for another hour. The sol was left to congeal in air for 72 h, and then heated in an oven at temperatures of up to 373 K for 7 days. The samples were calcinated at 923 K. They exhibited colour gradation from white – for undoped TiO_2, through yellow, to light brown – when the Fe_2O_3 content increased. The crystal structure of the materials was examined by means of X-ray diffraction conducted using a *Philips* X'Pert Pro MD diffractometer.

2.2. Cyclic voltammetry measurements

Electrochemical measurements – *cyclic voltammetry* (CV), *linear sweep voltammetry* (LSV), and *chronoamperometry* (CA) – were carried out with an M161 electrochemical analyzer (MTM-ANKO), at room temperature.

A conventional three-electrode system was applied, with a TiO_2–Fe_2O_3–Nafion modified glassy carbon electrode (TiO_2–Fe_2O_3–Nafion/GCE) as the working electrode, platinum wire as the auxiliary electrode, and Ag/AgCl as the reference electrode (Fig. 1). The GCE (3 mm diameter) was polished before the experiment with a 1.0 and 0.3 μm alumina powder, and then cleaned ultrasonically with distilled water and ethanol to remove trace amounts of contaminants. In a subsequent step, 10 μl of a TiO_2 and TiO_2–Fe_2O_3 powder dispersion (7.2 mg in 1 ml of Nafion)

was deposited on the pre-cleaned GCE and allowed to dry in air under ambient conditions. Cyclic voltammograms were recorded in 0.1 M NaOH upon the successive addition of hydrazine.
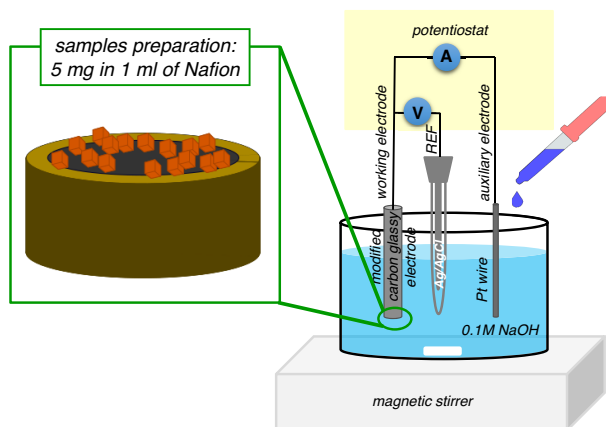

Fig. 1. Schematic illustration of cyclic voltammetry measurements system.

The electrochemically active surface area was determined using the Randles–Sevcik equation. Cyclic voltammograms for 1 mM of $K_3[Fe(CN)_6]$ in 0.1 M of KCl as a supporting electrolyte were then recorded at scan rates (v) varying from 25 to 500 mV/s.

3. Results and discussion

3.1. TiO$_2$–Fe$_2$O$_3$ powder characterization

The crystal structure and phase composition of titanium(IV) oxide modified with Fe_2O_3 were determined based on XRD studies. The analyzed diffraction patterns indicated that TiO_2 had crystallized as anatase. TiO_2 + 2 mol% of Fe_2O_3 materials are a mixture of two polymorphs of titanium dioxide, anatase and rutile. However, the anatase polymorphic form was predominant. In the case of the TiO_2 + 20 mol%Fe_2O_3 a contribution from pseudobrookite (Fe_2TiO_5) was also found. These results are consistent with the phase diagram for the TiO_2–Fe_2O_3 system proposed by MacChesney and Muan [32].

3.2. Electrochemical behaviour of GC electrodes modified with TiO$_2$–Fe$_2$O$_3$

To investigate the surface of the working electrode, the $Fe(CN)_6^{3-/4-}$ redox system and the Randles–Sevcik equation were used [33, 34]. The effect of applying different scan rates in the range from 25 to 500 mV/s with the analyzed GC electrodes modified with titania, investigated using a 0.1 M KCl solution containing 1 mM of $K_3[Fe(CN)_6]$, is shown in Fig. 2a; the corresponding current vs. $v^{0.5}$ plots are presented in Fig. 2b.

In the voltammograms recorded using the glassy carbon electrode modified with TiO_2 at different scan rates (Fig. 2a), two peaks – an anodic and a cathodic one, attributed to the presence of the ferricyanide/ferrocyanide redox couple – can be seen. According to the Randles–Sevcik equation:

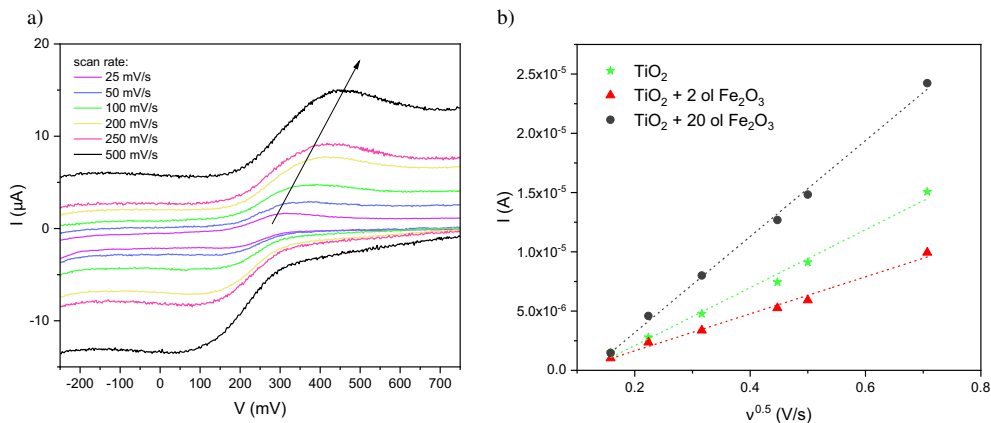$$I = 0.4463 \left(F^3RT^{-1}\right)^{0.5} A\, n^{1.5} D^{0.5} C_0 v^{0.5}, \tag{1}$$

a)

b)

Fig. 2. (a) CVs recorded for 0.1 M of KCl + 1 mM of K$_3$[Fe(CN)$_6$] using a GC electrode modified with TiO$_2$, at various scan rates; (b) peak current as a function of the square root of the scan rate.

where F is the Faraday constant (96485 C/mol), R is the gas constant (8.314 J/molK), A represents the electrochemically active surface area of the electrode (cm^2), I stands for current peak (A), n corresponds to the number of electrons involved in the redox reaction ($n = 1$), T is temperature (298 K), and D and C_0 represent the diffusion coefficient (7.2×10^{-6} cm^2/s) and concentration (1 mM) of K$_3$[Fe(CN)$_6$], respectively.

The active surface area can be calculated from the slope of I vs. $v^{0.5}$. The results revealed that TiO$_2$ + 20 mol% of Fe$_2$O$_3$ (5.62 mm^2) had the biggest active surface area while the composition with the 2 mol% of hematite (2.16 mm^2) had the smallest one. The active areas of sensors based on TiO$_2$+ Fe$_2$O$_3$ were smaller than the geometric surface of the electrode which may be responsible for the shape of voltammograms typical for microelectrodes. As the sensors tested do not meet the conditions for typical microelectrodes, their response can be described as multiplied. At the same time, for higher hydrazine concentrations, an increasing distortion of the recorded curves can be observed. This demonstrates the share of adsorption phenomena accompanying analyte oxidation in the studied environment.

Additionally, the half-wave potentials, for which the velocity of the electron transfer reaction equals the diffusion velocity, were determined. The results obtained are summarized in Fig. 3a. With the increase in hydrazine concentration, a shift in the half-wave potential towards positive potential values is observed. As a result of blocking the electrode surface, presumably by adsorption of the electrode reaction products, the redox reaction becomes more difficult. This means that higher energy is required to transfer the electron towards the electrode surface.

The electrochemical behaviour of glassy carbon electrodes modified with TiO$_2$–Fe$_2$O$_3$ in the absence and presence of hydrazine was evaluated via cyclic voltammetry (CV), in a 0.1 M NaOH electrolyte and in the potential window between –125 and 800 mV.

Figure 4 illustrates the voltammetric response of the prepared modified electrodes to different amounts of hydrazine. Strong oxidation peaks were observed in the case of all the samples – at 357 mV for TiO$_2$ (Fig. 4b), 327 mV TiO$_2$ + 2 mol% of Fe$_2$O$_3$ (Fig. 4c) and 391 mV for TiO$_2$ + 20 mol% of Fe$_2$O$_3$ (Fig. 4d). It is worth noting that no peaks were observed in the reverse scan. These results indicate the irreversible nature of the oxidation process, as expressed by the following reaction [35]:
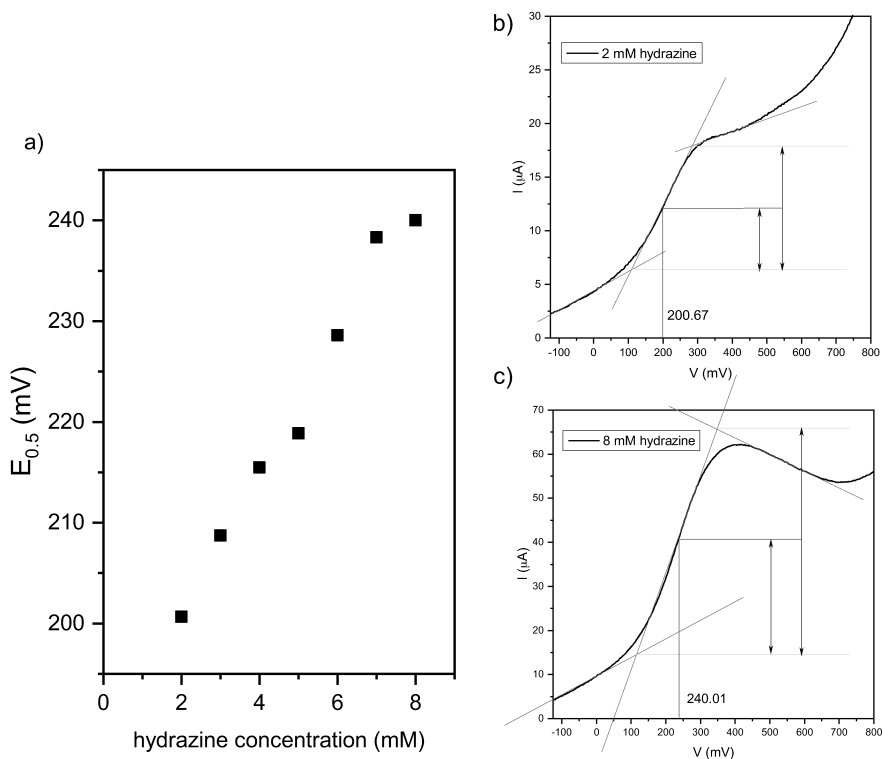
$$N_2H_4 \rightarrow N_2 + 4H^+ + 4e^-. \tag{2}$$

Fig. 3. (a) Half-wave potential vs hydrazine concentration for TiO_2–Nafion–GCE electrode with the examples of determination of half-wave potential for (b) 2 mM and (c) 8 mM hydrazine.

However, some authors postulate that the performance of the electrochemical hydrazine sensor is determined by the catalytic reaction that is associated with the presence of hydroxyl groups [36, 37]:

$$N_2H_4 + 4OH^- \rightarrow N_2 + 4H_2O + 4e^-. \tag{3}$$
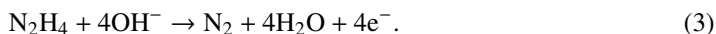
Up to about 5 mM of N_2H_4 CV voltammograms have a typical "sigmoid" shape for micro-electrodes. However, the sensor used is not a microelectrode (GCE diameter is 3 mm), so the effect comes from many active centres on the surface of the studied system. At the same time, for higher hydrazine concentrations, an increasing distortion of the recorded curves can be observed. This demonstrates the share of adsorption phenomena accompanying analyte oxidation in the studied environment.

An analysis of the peak shape also provides information about electron transfer. According to Zhao *et al.* [38], a sharp and well-defined signal can be attributed to a high reaction rate. The obtained data showed that for 2 mol% of Fe_2O_3, the oxidation potential of hydrazine was lower than in the case of the other modified electrodes. This may suggest an effectively reduced diffusion layer and improved electron transfer between the electrode and hydrazine.

In order to investigate the electrocatalytic properties of a TiO_2–Fe_2O_3/Nafion/GCE sensor, typical amperometric (I vs. t) response measurements upon the successive addition of hydrazine at potentials determined from the CV curves in Fig. 4 were carried out (Fig. 5). The results showed that the investigated modified glassy carbon electrodes exhibit a rapid and sensitive response
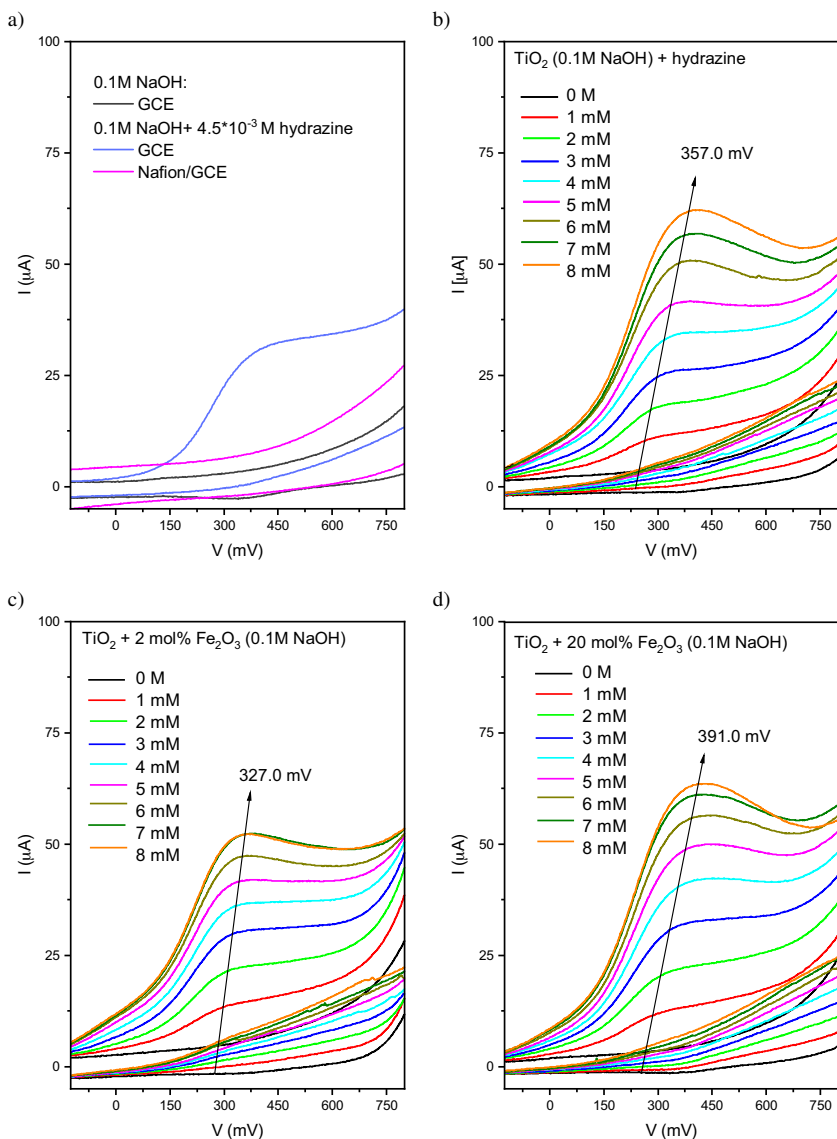
Fig. 4. Cyclic voltammograms recorded for bare glassy carbon (GCE) and Nafion modified GCE (Nafion/GCE) in presence N₂H₄ (a) and different concentrations of hydrazine using GC electrodes modified with: (b) TiO₂, (c) TiO₂ + 2 mol% of Fe₂O₃ and (d) TiO₂ + 20 mol% of Fe₂O₃; scan rate – 50 mV/s, supporting electrolyte – 0.1 M NaOH.

upon each introduction of hydrazine, indicating that the TiO₂–Fe₂O₃ coupled system undergoes a strongly enhanced oxidation reaction.

Based on the obtained data, it can be assumed that surface development has little influence on the sensor's reactivity towards hydrazine and the enhancement of sensing capability correlates with the formed electronic heterostructure and the amount of hematite in the composition. Moreover, these results indicate that the kinetics of the electrochemical reaction is controlled by the specific surface adsorption of hydrazine.
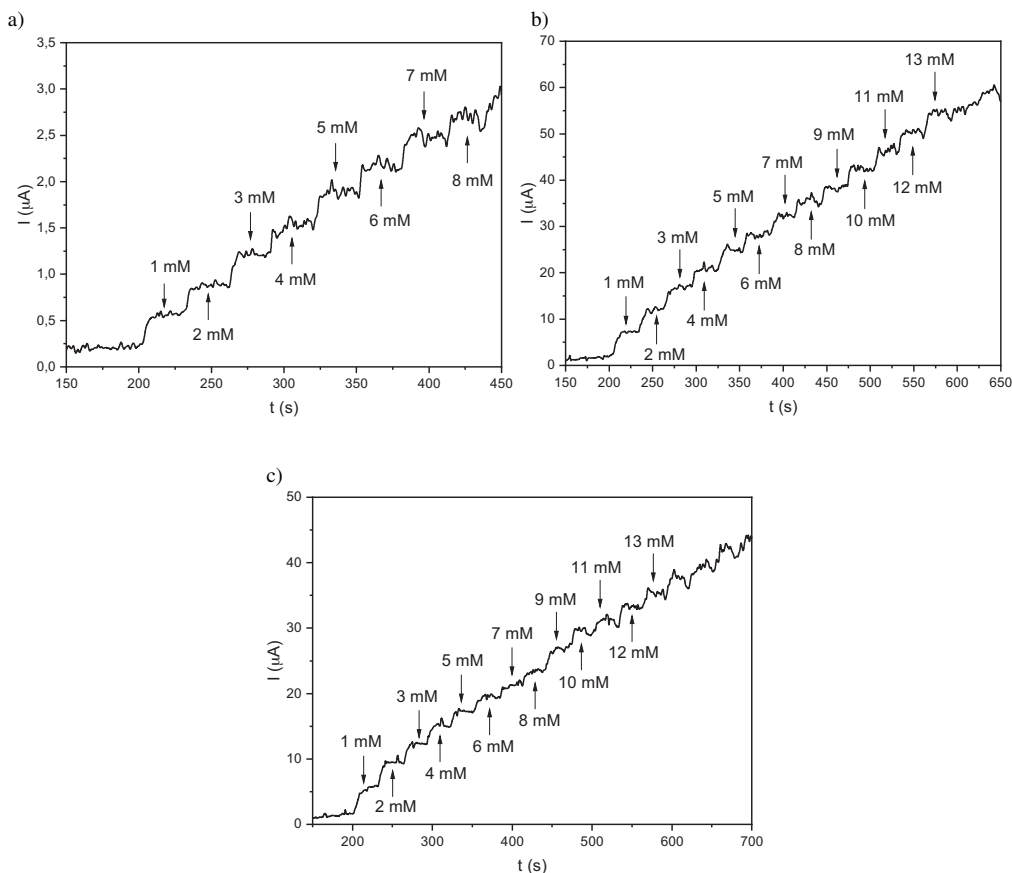
PAN

Metrol. Meas. Syst., Vol. 27 (2020), No. 2, pp. 301–311

DOI: 10.24425/mms.2020.132776

POLSKA AKADEMIA NAUK

Fig. 5. Amperometry response recorded by means of GC electrodes modified with (a) TiO_2, (b) $TiO_2 + 2$ mol% of Fe_2O_3 and (c) $TiO_2 + 20$ mol% of Fe_2O_3 upon subsequent additions of hydrazine; electrolyte – 0.1 M NaOH, applied potential – 364, 327 and 391 mV for a, b and c, respectively.

The calibration curves for different concentrations of hydrazine, at potentials defined by the characteristics of the CVs in Fig. 5, are shown in Fig. 6a. The sensitivity of the modified GC electrodes, expressed in terms of the limit of detection (*LOD*) and limit of quantification (*LOQ*), was calculated based on these curves. The relationship between the *LOD* and the *LOQ* may be expressed in the form of the following equation [39]:

$$LOD/LOQ = \frac{f \cdot SD}{b}, \tag{4}$$

where f is the correlation factor equal to 3.3 for the *LOD* and 10 for the *LOQ*, *SD* represents the standard deviation of linear regression, and b stands for the slope of the regression line.

These two factors are used to describe the smallest concentration of the analyte (herein hydrazine) that can be measured with sufficient reliability using an analytical procedure. The data calculated for the GCEs modified with TiO_2–Fe_2O_3 are presented in Fig. 6b. It can be seen that the lowest values of *LOD* (0.13 mM) and *LOQ* (0.39 mM), and, thereby the best response, were obtained for the sample containing 2 mol% of hematite. It can be assumed that the incorporation of
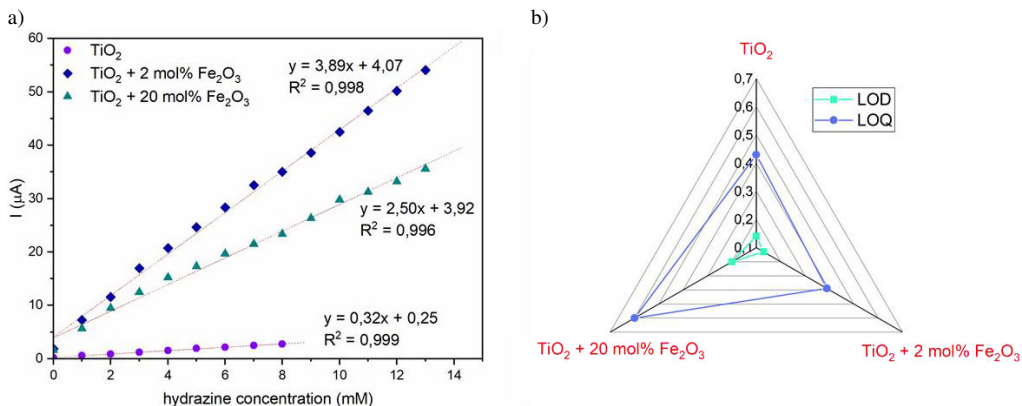
a)

b)

Fig. 6. (a) Calibration curves corresponding to hydrazine concentration vs. peak current and (b) the calculated limits of detection (*LOD*) and quantification (*LOQ*) for glassy carbon electrodes modified with TiO₂, TiO₂ + 2 mol% of Fe₂O₃ and TiO₂ + 20 mol% of Fe₂O₃.

iron(III) oxide enhances the sensor's sensitivity toward hydrazine. On the other hand, modification with TiO₂ + 20 mol% of Fe₂O₃ yields higher detection (0.20 mM) and quantification (0.60 mM) limits. This leads to the conclusion that there is a maximum concentration of hematite that improves the response of the sensor, and that this value is in the range from 2 to 20 mol%.

4. Conclusions

TiO₂–Fe₂O₃ powders were successfully synthesized by means of the sol-gel technique. GCEs modified with TiO₂–Fe₂O₃ were prepared by depositing 10 µl of a 7.2 mg/ml Nafion/powder suspensions on the electrode and allowing them to dry at room temperature.

The active surface area ($A_{TiO_2+20\%mol\ Fe_2O_3} > A_{TiO_2} > A_{TiO_2+2\%mol\ Fe_2O_3}$) may be responsible for multiplied "microelectrode effect". The analysis of the half-wave potential reveals that electron transfer is determined by the adsorption processes.

The electrocatalytic response of the prepared electrodes to hydrazine was determined in 0.1 M NaOH. It was found that anodic peak current increases together with the concentration of hydrazine. The results indicate the irreversible nature of the hydrazine oxidation process.

Experimental results also suggest that the formation of the TiO₂–Fe₂O₃ coupled system enhances electrochemical catalytic performance with regard to hydrazine detection. The modification TiO₂ + 2 mol% Fe₂O₃ provides good analytical performance of detection (0.13 mM) and quantification limits (0.39 mM). The presented TiO₂–Fe₂O₃ coupled system provides the premise for a suitable material for a stable, sensitive, and easy-to-use hydrazine sensor.

Acknowledgements

References

[1] Zargar, B., Hatamie, A. (2013). A simple and fast colorimetric method for detection of hydrazine in water samples based on formation of gold nanoparticles as colorimetric probe. *Sensors and Actuators B: Chemical*, 182, 706–710.

[2] Kim, S.K., Jeong, Y.N., Ahmed, M.S., You, J.-M, Choi, H.C., Jeon, S. (2011). Electrocatalytic determination of hydrazine by a glassy carbon electrode modified with PEDOP/MWCNTs-Pd nanoparticles. *Sensors and Actuators B: Chemical*, 153, 246–251.

[3] He, Y., Hang, W., Liang, Y., Yu, H. (2015). A low-cost and label-free assay for hydrazine using MnO_2 nanosheets as colorimetric probes. *Sensors and Actuators B: Chemical*, 220, 927–931.

[4] Choudhary, G., Hansen, H. (1998). Human health perspective on environmental exposure to hydrazines: a review. *Chemosphere*, 37(5), 801–843.

[5] Kim, S.P., Choi, H.C. (2015). Reusable hydrazine amperometric sensor based on Nafion®-coated TiO_2-carbon nanotube modified electrode. *Sensors and Actuators B: Chemical*, 207, 424–429.

[6] Moghaddam, H.M., Beitollahi, H., Tajik, S., Sheikhshoaie, I., Biparva, P. (2015). Fabrication of oval TiO_2 nanoparticles/Mn(III) salen doped carbon paste electrode: application as electrochemical sensor for determination of hydrazine in the presence of phenol. *Environmental Monitoring and Assessment*, 187(7).

[7] Kumar, A., Burns, J., Hoffmann, W., Demattio, H., Malik, A.K., Matysik, F.M. (2011). Determination of hydrazines by chip electrophoresis with contactless conductivity detection. *Electrophoresis*, 32(1), 920–925.

[8] Ganesh, S., Khan, F., Ahmed, M.K., Pandey. S.K. (2011). Potentiometric determination of free acidity in presence of hydrolysable ions and sequential determination of hydrazine. *Talanta*, 85(1), 958–963.

[9] George, M., Nagaraja, K.S., Balasubramanian, N. (2008). Spectrophotometric determination of hydrazine. *Talanta*, 75(1), 27–31.

[10] Safavi, A., Karimi, M.A. (2002). Flow injection chemiluminescence determination of hydrazine by oxidation with chlorinated isocyanurates. *Talanta*, 58(3), 785–792.

[11] Gilbert, R., Rioux, R., Saheb, S.E. (1984). Ion chromatographic determination of morpholine and cyclohexylamine in aqueous solutions containing ammonia and hydrazine. *Analytical Chemistry*, 56(1), 106–109.

[12] Mori, M., Tanaka, K., Xu, Q., Ikedo, M., Taoda, H., Hu, W. (2004). Highly sensitive determination of hydrazine ion by ion-exclusion chromatography with ion-exchange enhancement of conductivity detection. *Journal of Chromatography A*, 1039(1–2), 135–139.

[13] Ahmad, R., Tripathy, N., Ahn, M.S., Hahn, Y.B. (2017). Highly stable hydrazine chemical sensor based on vertically-aligned ZnO nanorods grown n electrode. *Journal of Colloid and Interface Science*, 494, 153–158.

[14] Dong, Y., Yang, Z., Sheng, Q., Zheng, J. (2018). Solvothermal synthesis of Ag@Fe_3O_4 nanosphere and its application as hydrazine sensor. *Colloids and Surfaces A*, 538, 371–377.

[15] Yang, Z., Sheng, Q., Zhang, S., Zheng, X., Zheng, J. (2017). One-pot synthesis of Fe_3O_4/polypyrrole/graphene oxide nanocomposites for electrochemical sensing of hydrazine. *Micromchim Acta*, 184(7), 2219–2226.

[16] Yang, Y.J., Li, W., Wu, X. (2014). Copper sulfide reduced Graphene oxide nanocomposite for detection of hydrazine and hydrogen peroxide at low potential in neutral medium. *Electrochimica Acta*, 123, 260–267.

[17] Harraz, F.A., Ismail, A.A., Al-Sayari, S.A., Al-Hajry, A., Al-Assiri, M.S. (2016). Highly sensitive amperometric hydrazine sensor based on novel α-Fe$_3$O$_3$/crosslinked nanocomposite modified glassy carbon electrode. *Sensors and Actuators B: Chemical*, 234, 573–582.

[18] Ameen, S., Akhtar, M.S., Shin, H.S. (2012). Hydrazine chemical sensing by modified electrode based on *in situ* electrochemically synthesized polyaniline/graphene composite thin film. *Sensors and Actuators B: Chemical*, 173, 177–183.

[19] Li, J., Xie, H., Chen, L. (2011). A sensitive hydrazine electrochemical sensor based on electrodeposition of gold nanoparticles on choline film modified glassy carbon electrode. *Sensors and Actuators B: Chemical*, 153, 239–245.

[20] Nassef, H.M., Radi, A.-E., O'Sullivan, C.K. (2006). Electrocatalytic oxidation of hydrazine at *o*-aminophnol grafted modified glassy carbon electrode: Reusable hydrazine amperometric sensor. *Journal of Electroanalytical Chemistry*, 592(1), 139–146.

[21] Li, C., Li, M., Bo, X., Y, L., Mtukula, A.C., Guo, L. (2016). Facile synthesis of electrospinning Mn$_2$O$_3$-Fe$_2$O$_3$ loaded carbon fibers for electrocatalysis of hydrogen peroxide reduction and hydrazine oxidation. *Electrochim. Acta*, 211, 255–264.

[22] Shykla, S, Chaudhary, S., Umar, A., Chaudhary, G.R., Mehta, S.K. (2014). Tungsten oxide (WO$_3$) nanoparticles as scaffold for the fabrication of hydrazine chemical sensor. *Sensors and Actuators B: Chemical*, 196, 231–237.

[23] Zhang, J., Liu, H., Dou, M., Wang, F., Liu, J., Li, Z., Ji, J. (2015). Synthesis and characterization of Co$_3$O$_4$/multiwalled carbon nanotubes nanocomposite for amperometric sensing of hydrazine. *Electroanalysis*, 27(5), 1188–1194.

[24] Khan, S.B., Faisal, M., Rahman, M.M., Abdel-Latif, I.A., Ismail, A.A., Akhtar, K., Al-Hajry, A., Asiri, A.M., Alamry, K.A. (2013). Highly sensitive and stable phenyl hydrazine chemical sensors based on CuO flower shapes and hollow spheres. *New Journal of Chemistry*, 37(3), 1098–1104.

[25] Wang, G., Zhang, C., He X., Li, Z., Zhang, X., Wang, L., Fang, B. (2010). Detection of hydrazine based on Nano-Au deposited on Porous-TiO$_2$ film. *Electrochimica Acta*, 55(24), 7204–7210.

[26] Ameen, S. Akhtar, M.S., Seo, H.-K., Shin, H.-S. (2013). TiO$_2$ nanotube arrays *via* electrochemical anodic oxidation: Prospective electrode for sensing phenyl hydrazine. *Applied Physics Letters*, 103(06), 061602.

[27] Ojani, R., Safshekan, S., Raoof, J.-B. (2014). Photoelectrochemical oxidation of hydrazine on TiO$_2$ modified titanium electrode; its application for detection of hydrazine. *Journal of Solid State Electrochemistry*, 18(2), 779–783.

[28] Yi, Q., Niu, F., Yu, W. (2011). Pd-modified TiO$_2$ electrode for electrochemical oxidation of hydrazine, formaldehyde and glucose. *Thin Solid Films*, 519(10), 3155-3161.

[29] Dong, B., He, B.-L., Huang, J., Gao, G.-Y., Yang, Z., Li, H.-L. (2008). High dispersion and electrocatalytic activity of Pd/titanium dioxide nanotubes catalysts for hydrazine oxidation. *J. Power Sources*, 175(1), 266–271.

[30] Yang, Z., Zheng, X., Zheng, J. (2017). MnCo$_2$S$_4$ nanoparticle-assembled hierarchical porous sphere as an effective electrocatalyst for highly sensitive and selective nonenzymatic detection of hydrazine. *Sensors and Actuators B: Chemical*, 253, 34–41.

[31] Kundu, T.K., Mukherjee, M., Chakravorty, D. (1998). Growth of nano-α-Fe$_2$O$_3$ in a titania matrix by the sol-gel route. *Journal of Materials Science*, 33(7), 1759–1763.

[32] MacChesney, J.B., Muan, A. (1959). Studies in the system iron oxide-titanium oxide. *American Mineralogist: Journal of Earth and Planetary Materials*, 44(9–10), 926–945.

[33] Abolhasani, J., Hosseini, H., Khanmiri, R.H. (2014). Electrochemical study and differential pulse voltammetric determination of oxcarbazepine and its main metabolite at a glassy carbon electrode. *Analytical Methods*, 6(2), 850–856.

[34] Ngamchuea, K., Eloul, S., Tschulik, K., Compton, R.G. (2014). Planar diffusion to macro disc electrodes what electrode size is required for the Cottrel and Randles–Sevcik equations to apply quantitatively? *Journal of Solid State Electrochemistry*, 18(12), 3251–3257.

[35] Tang, Y.Y., Kao, C.L., Chen, P.Y. (2012). Electrochemical detection of hydrazine using a highly sensitive nanoporous gold electrode. *Analytica Chimica Acta*, 711, 32–39.

[36] Rosca, V., Koper, M.T.M. (2008) Electrocatalytic oxidation of hydrazine on platinium electrodes in alkaline solutions. *Electrochim. Acta*, 53, 5199–5205.

[37] Sultana, W., Eraiah, B., Vasan, H. (2012). Efficient polyglycine modified Au electrode for the detection of hydrazine. *Analytical Methods*, 4(12), 4115–4120.

[38] Zhao, Z., Wang, Y., Li, P., Sang, S., Zhang, W., Hu, J., Lian, K. (2015). A highly sensitive electrochemical sensor based on Cu/Cu_2O@carbon nanocomposite structures for hydrazine detection. *Analytical Methods*, 7(21), 9040–9046,

[39] Shrivastava, A., Gupta, V. (2011). Methods for the determination of limit of detection and limit of quantification of the analytical methods. *Chronicles of Young Scientists*, 2(1), 21–25.